The Gross Structure of Reaction Mechanism in Multi—Particle Production Process

Hujio Noda

Department of Physics, Ibaraki University, Mito

1. Introduction

We investigate the structure of high energy hadron-hadron interaction. We treat the multi-particle production process from such a viewpoint that the reaction mechanism is composed of the non-diffractive (ND) mechanism and the diffractive (D) mechanism.[1)•)] We analyze the data by means of a model calculation.[2)] The D and ND are specified by whether the so-called Pomeron is exchanged somewhere in a multi-peripheral chain or not, respectively. The Pomeron used in this report is not necessarily equivalent to the one exchanged in elastic channel. The question what this Pomeron is, may be remined in future but it may be a dynamical object which plays an important role in high energy hadron-hadron interaction.

Here, we shall clarify following points : When the final multuplicity is fixed, a dominant reaction mechanism of the production process switches over from ND to D mechanism with increasing energy. On the other hand, the former (or the latter) is dominant in reactions with large (or small) multiplicity at a fixed incident energy. It is shown that the structure of the reaction mechanism is characterized on the multiplicity-incident momentum plane.

•) Recently, two representative models ; the multi-peripheral model[3)] and the deffractive excitation (fragmentation) model,[4),5)] have been investigated extensively by many theorists for the reaction mechanism of multi-particle production process. As these thoughts are monistic, they explain only the partial features of experiments and faced with difficulties in essential points.[6)]

2. Reaction mechanism of exclusive reactions

Multi-peripheral mechanism

We consider the following reaction with multiplicity n :

$$a + b \rightarrow c_1 + c_2 + \cdots\cdots + c_n \qquad (2-1)$$

where a and b are initial particles and c_i's are final particles. We assume the multi-peripheral mechanism as the basic one in multi-particle production. We denote the four momenta of the particles a, b and c_i as P_a, P_b and q_i, respectively. The number i represents the order from the side of particle a in multi-peripheral chain and the invariant variables are defined as follows :

$$s = (P_a + P_b)^2, \; t_j = (P_a - \sum_{i=1}^{j} q_i)^2, \; s_j = (q_{j+1} + q_j)^2$$

There, we neglect the spins and iso-spins of the particles for simplicity.

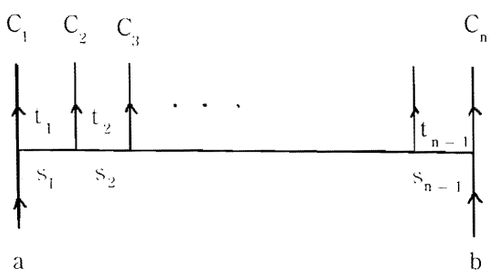

Matter and Pomeron

We can classify the objects exchaged in multi-peripheral chain into two categories : matter and Pomeron. Mesons and baryons belong to matter, and Pomeron is a object with vacuum quantum number. Here, we assume that the effective amplitude takes the following forms for the exchange of matter and the one of Pomeron in multi-peripheral chain :

(A) $e^{a t_i} (\frac{s_i}{s_0})^{\alpha_M}$ for matter, where $a = 2$ (Gev/c)$^{-2}$ and $\alpha_M \simeq 0$,

(B) $e^{b t_j} (\frac{s_j}{s_0})^{\alpha_P}$ for Pomeron, where $b = 8$ (Gev/c)$^{-2}$ and $\alpha_P \simeq 1.0$

Where s_0 is scaling parameter and is taken to be 1 (Gev/c).[2]

General scheme

We divide the amplitude for the reaction (2-1) into the non-diffractive and diffractive parts. Namely, the amplitude T_n is written as

$$T_n = T_n^{ND} + T_n^{D} \qquad (2-2)$$

where T_n^{ND} and T_n^{D} denote the amplitudes of ND and D mechanism, respectively. The ND mechanism is specified by such a mechanism that Pomeron is exchanged nowhere in multi-peripheral chain. The D mechanism is characterized by the existence of Pomeron exchange in the one. The number of exchanged Pomeron may increase in high energies, since its dynamical threshold becomes high for the sake of the structure of Pomeron. It is noted that all reactions have not necessarily the two mechanism. For example, the D mechanism is forbidden for the process $K^- p \rightarrow \pi\pi\pi\Lambda$.

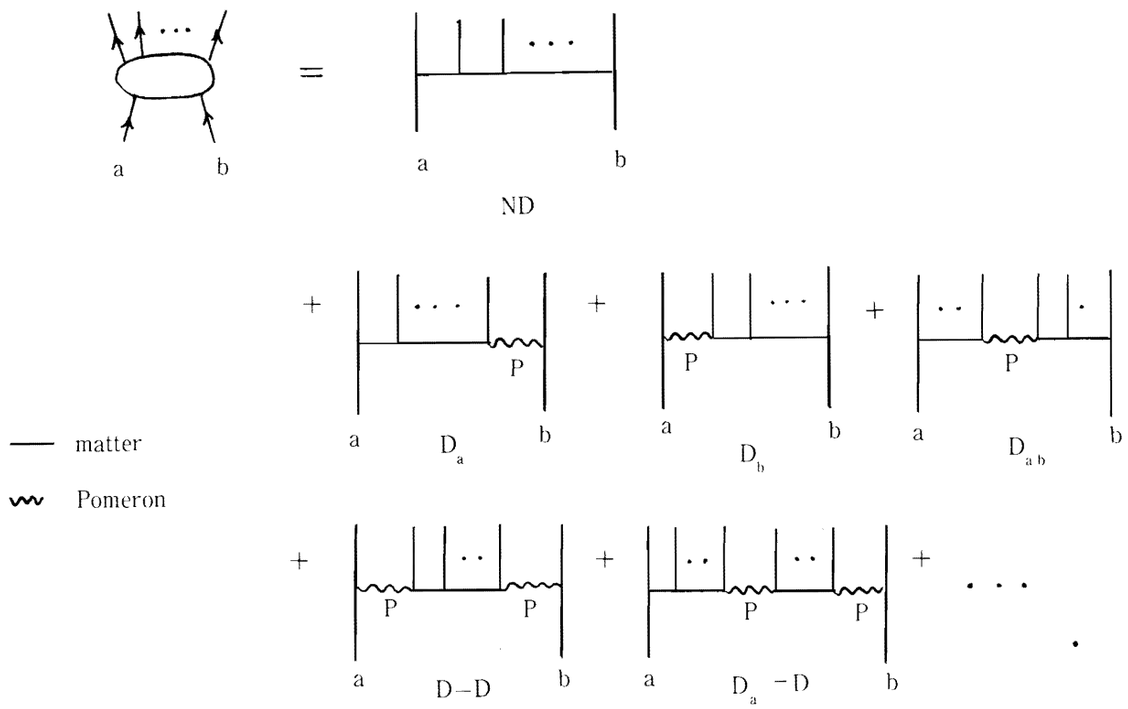

We parametrize the amplitudes T_n^{ND} and T_n^{D} as follows :

$$T_n^{ND} = C_n \cdot C^{ND} \prod_{i=1}^{n-1} e^{a t_i}$$

$$T_n^{D} = C_n \cdot C^{Dk} \prod_{i=1}^{k-1} e^{a t_i} \cdot \left(\frac{S_k}{S_0}\right)^{\alpha_P(0)t_i} \cdot \prod_{j=k+1}^{n-1} e^{a_j t_j} + \cdots\cdots\cdots$$

where C_n is a normalization constant which is free from any mechanism but depends on n, and C^{ND} and C^{Dk} are relative weights of the respective mechanism and are assumed to be independent of n, for simplicity. The sum over k is taken only for the terms which Pomeron exchange is allowed in multi-peripheral chain. We use the following relative weights for three mechanisms :

$$C^{ND} : C^{DN} : C^{D\pi} = 8 : 2 : 1.3 \qquad (2-3)$$

3. Partial cross sections

We analyze the partial cross section ($\sigma_n(s)$) for the following reactions[7] in order to investigate the energy dependence of cross section and the role of the ND and D mechanism :

$$\begin{aligned} \pi^- p &\to \pi^- \pi^0 p \\ &\to \pi^- \pi^+ \pi^- p \\ &\to \pi^- \pi^+ \pi^- \pi^0 p \\ &\to \pi^- \pi^+ \pi^- \pi^+ \pi^- p \end{aligned} \qquad (3-1)$$

Their amplitudes are

$$T_3 = T_3^{ND} + T_3^{DN}$$

$$T_4 = T_4^{ND} + T_4^{DN} + T_4^{D\pi} + T_4^{D-D}$$

$$T_5 = T_5^{ND} + T_5^{DN} + T_5^{D\pi N}$$

$$T_6 = T_6^{ND} + T_6^{DN} + T_6^{D\pi} + T_6^{D\pi N} + T_6^{D-D}$$

Then we neglect the $D_{\pi N}$ and D–D mechanism, since we treat these reactions in the energy region from threshold to $P_L \simeq 100$ GeV/c. The fits are shown in Fig. 1.

From this analysis, the following results can be derived : The ND cross section rises steeply from threshold, reaches the maximum point and then decreases as $P_L^{-\nu}$ ($\nu \simeq 2.0$). On the other hand, those of D_N and D_π rises slowly from threshold and approaches to a constant behaviour with increasing energy. The gross behaviour of each mechanism is as follows :

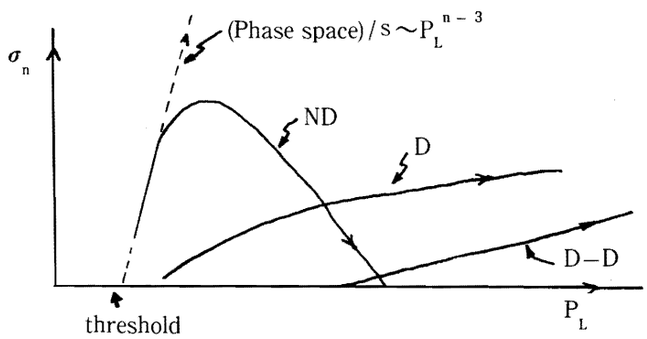

When we look out over the whole exclusive reactions, it is seen that the gross feature of them is characterized by the various areas on the multiplicity-incident momentum plane as follows :

Region (I) : The energy region is from the threshold to the point slightly beyond the energy corresponding to the maximum peak of σ_n (s). In this region the ND type mechanism dominate : $\sigma_n^{ND} > \sigma_n^{D}$.

Region (II) : Here σ_n (s) is attributed to both ND and D mechanism with a comparable order : $\sigma_n^{ND} \sim \sigma_n^{D}$

Region (III) : The high energy region where σ_n (s) comes mainly from the D type : $\sigma_n^{D} > \sigma_n^{ND}$

We sketch such a feature in Fig. 2 on the multiplicity-incident momentum plane. The regions (I), (II) and (III) construct a band scheme. With increasing energy, it becomes easier to separate the D mechanism from the ND mechanism. Also, it is noted the following hierarchy :

$$\sigma_n^{D\pi}(s) > \sigma_n^{DN}(s)$$

This comes from the mass effect of proton.

Threshold peak

We call the maximum point of the cross section as the threshold peak. We discuss the importance of the above viewpoint. Yap Sue-Pin etal.[8] and T. Morii and the present author[1] analyzed the experimental data of J.D. Hansen et al.[9] by the universal t_i-cut mechanism and showed that the empirical formula,

$$P_n^{max.} = an^b$$

between the multiplicity (n) and the momentum ($P_n^{max.}$) corresponding to the maximum point of σ_n (s), is explained by the universal t_i-cut mechanism as shown in Fig. 3. This result is understood as follows : The maximum point of σ_n (s) belongs to region (I) and therefore the main part of σ_n (s) comes from the ND mechanism i.e. the universal t_i-cut mechanism. Also, the t_i-cut mechanism exhibits the rank structure of the cross section at the threshold peak[10] as shown in Fig. 4.

Development of D mechanism

We consider how much ratio the cross section of D type occupies in σ_n (s) at a fixed s. The ratio is presented in Fig. 5. The ratio becomes large and small as the energy increases at the small and large multiplicities, respectively. The D mechanism is an important mechanism, especially for the particle correlation such as the dispersion of the multiplicity and for the forward-backward asymmetry as disscussed in the following section.

4. Missing mass distributions

We study the missing mass distribution of exclusive reactions in order to check the validity of the results in 3. There are no data of missing mass distributions for the reaction considered in 3. We use the one with fixed number of pions in the process $\pi^- p \to \pi_f^-$ $(m\pi + N)^+$ for m = 1, 2, 3 and 4, where π_f^- is a leading particle.[11]

Development of the N* spectrum

We consider the development of the N* spectrum by the D_N mechanism. The N* spectrum, as shown in Fig. 6, exhibits the energy independence from the region (II), which corresponds the nearly constant behaviour of σ_n^{DN}. The diffractive excitation spectrum is well known at PS energy for the small multiplicity. If one would like to detect the diffractive excitation spectrum with high mass, a 200 GeV energy may be need at least. So it seems to be possible at NAL.

The incident momentum points for the model calculation are as follows :

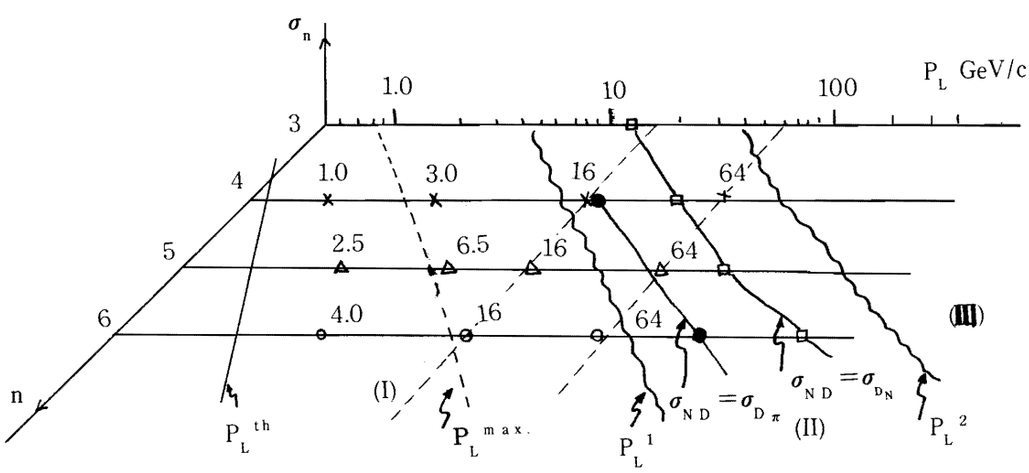

It is noted that the N^* spectrum nearly exhibits the similar structure at the same regions on the multiplicity-incident momentum plane. The similar structures appear in the ND and Dπ mechanism as shown in Fig. 7 and 8. These results support the band scheme.

Fits

We analyze experimental data at $P_L = 16$ GeV/c. We take the value of (2–3) for the relative weights C^{ND}, C^{D_N} and $C^{D\pi}$ and the results by our model are shown by the solid lines in Fig. 9. Our results give a good agreement with data except for the case of m = 3. It may be necessary to confirm this experimental data of $\pi^- p \to \pi^-{}_f (3\pi N)^+$.

5. Forward-backward asymmetry and reaction mechanism

Until now, we have discussed the cross section and the missing mass distibution of exclusive reaction and investigated the gross structure of reaction mechanisms ; i.e. ND and D mechanism for them.

In this section, we consider the forward-backward asymmetry in the center of mass system.

We consider the following reaction :

$$\underbrace{a + b \to c_1 + c_2 + \ldots\ldots + c_i}_{n_+} + \underbrace{c_{i+1} + \ldots\ldots + c_n}_{n_-}$$

forward production　　backward production

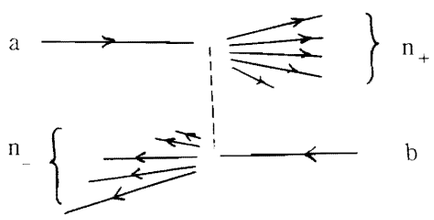

where n_+ and n_- denote the number of particles produced in the forward and backward direction, respectively. Then, the total number n is $(n_+ + n_-)$. Its cross section is represented by $\sigma_n^{(n_+, n_-)}$. We have the following relation between cross sections $\sigma_n^{(n_+, n_-)}$ and the partial cross section σ_n :

$$\sigma_n = \sum_{n_+} \sigma_n^{(n_+, n_-)} \qquad 5\text{–}1)$$

Data

We show the experimental data of $\sigma_n^{(n_+, n_-)}$ in Fig. 10.

It is noted that $\sigma_n^{(n_+, n_-)}$ of the reaction $\pi^- p \to \pi^- \pi^+ \pi^- \pi^+ \pi^- p$[12] has the peak at $n_+ = 3$ and its energy dependence exhibits the behaviour of the increase and decrease from $P_L = 5$ GeV/c to 16 GeV/c. Also, at the both sides the cross section increase. On the other hand, $\sigma_n^{(n_+, n_-)}$ of pp at 28 GeV/c[13] shows the V-type shape and the production of particles has the forward-backward asymmetry.

Definition of asymmetry

We consider the following quantities to characterize the forward-backward asymmetry for the n-particle production :

$$\bar{A}_n \equiv \sum_{n_+} A_n \sigma_n^{(n_+, n_-)} / \sigma_n \qquad (5\text{–}2)$$

where $\Delta_n \equiv n_+ - n_- = 2(n_+ - \frac{n}{2})$.

Also, we may extend it to the inclusive value as follows :

$$\bar{\Delta} \cdot \sigma_T = \sum_n^\infty \bar{\Delta}_n \cdot \sigma_n = \sum_n^\infty \sum_{n_+}^{n-1} \Delta_n \sigma_n^{(n_+, n_-)}).$$

Similarly, we define the absolute asymmetry as follows :

$$\begin{aligned} |\Delta_n| &\equiv |n_+ - n_-| \ , \\ |\bar{\Delta}_n| &\equiv \sum_{n_+} |\Delta_n| \sigma_n^{(n_+, n_-)} / \sigma_n \qquad -n \\ |\bar{\Delta}| \cdot \sigma_T &= \sum_n^\infty |\bar{\Delta}_n| \cdot \sigma_n \end{aligned} \tag{5-3}$$

Reaction mechanism and $\sigma_n^{(n_+, n_-)}$

We show the model calculation of $\sigma_n^{(n_+, n_-)}$ for the reaction $\pi^- p \to \pi^- \pi^+ \pi^- p$ at 16 GeV/c and 64 GeV/c in Fig. 11.

We have the results : the ND mechanism has one peak around $|\Delta_n| \simeq 0$, while the D mechanism (D_a and/or D_b) has one peak at $\Delta_n \neq 0$.

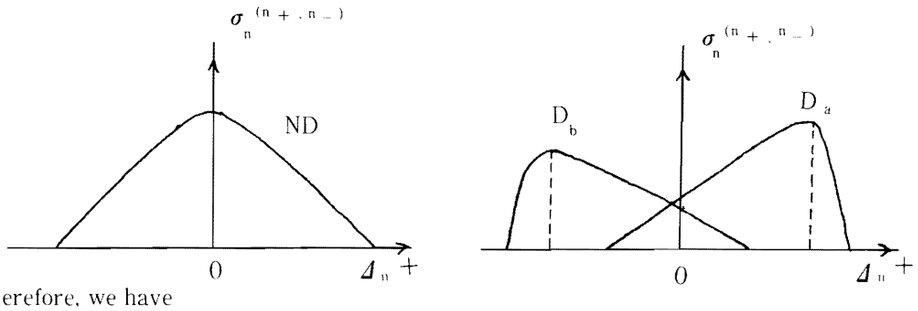

Therefore, we have

$$\begin{aligned} &\bar{\Delta}_n \text{ (ND)} \sim \text{small} \ , \\ &\bar{\Delta}_n \text{ (D)} \sim \text{large} \ . \end{aligned} \tag{5-4}$$

The data of $\pi^- p \to \pi^- \pi^+ \pi^- \pi^+ \pi^- p$ are understood as follows : The energy dependence of the peak at $n_+ = 3$ ($\Delta_6 = 0$) is characterized by the ND mechanism and the energy increase of $\sigma_n^{(n_+, n_-)}$ at both sides by the D mechanism (D_π and D_N) as shown in Fig. 1-(d). When the D mechanism dominates (Region III), $\sigma_n^{(n_+, n_-)}$ exhibits the V-type behaviour as the reaction of pp at 28 GeV/c.

X_i-distribution

The forward-backward asymmetry discussed above, is closely related to the longitudinal distribution as follows :

$$\bar{\Delta}_n \cdot \sigma_n = \sum_i \left\{ \int_0^{+1} \frac{d\sigma_n}{dx_i} dx_i - \int_{-1}^{0} \frac{d\sigma_n}{dx_i} dx_i \right\}$$

where $\frac{d\sigma_n}{dx_i}$ denotes the single-particle distribution of the i-th particle in the n-particle production and $x_i \equiv 2q_{1i} / \sqrt{s}$.

We show the x_i-distribution of each mechanism of $\pi^- p \to \pi^- \pi^+ \pi^- p$ at 27 GeV/c, for example, in Fig. 12. We may easily understand the results of (5-4). In general, we have the following results :

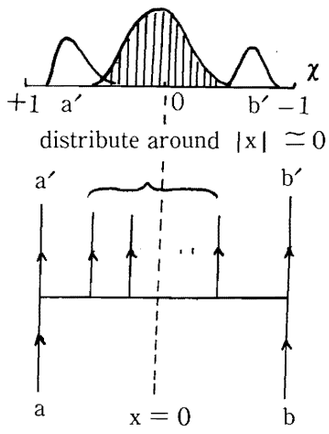

ND mechanism

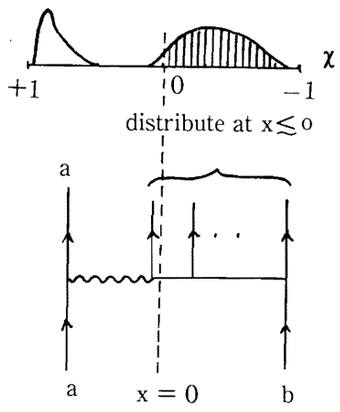

D_b mechanism

Separation of reaction mechanism

We present here a model calculation for the two-particle distribution of the reaction $\pi^- p \to \pi^- \pi^+ \pi^- p$. Its aim is to investigate the separation of reaction mechamism. We give $\frac{d^2\sigma_4}{dx_2\, dx_3}$ of the two particles produced in the central region in Fig. 13. These results seem to be consistent with the analysis of the LPS plots for 4-body reactions[14], but it seems to be uncorrect to conclude that the D mechanism is completely separated from the ND mechanism at 16 GeV/c, as shown in Fig. 14.

Finally, we emphasize that the energy dependence of $\bar{\Delta}_n$ and /or $\bar{\Delta}$ gives us the knowledge of the role of the D mechanism similar to f^2 and /or $D (\equiv \sqrt{<n^2> - <n>^2})$ at high energies.

6. Concluding remarks

We have investigate the role of ND and D mechanism and the energy behaviour of the relative magnitude of them and clarified the gross structure of exclusive reactions with a fixed multiplicity, in the energy region from threshold to $P_L \simeq 100$ GeV/c. The structure of high energy hadron-hadron interaction is prescribed by the one of matter and Pomeron. Thus, we should investigate the quality of them in more detail.

Also, in this report we assumed the ND mechanism is effectively composed of only one term. The ND mechanism, however, has to be divided into $\bar{X}$ and $\bar{H}$-type mechanism taking the urbaryon rearrangement diagram into account[15]. The $\bar{X}$-type mechanism may be dominant, since the sum of the cross sections of the $\bar{H}$-type mechanism must decrease like $s^{-\frac{1}{2}}$ by the reduction rule of urbaryon lines.

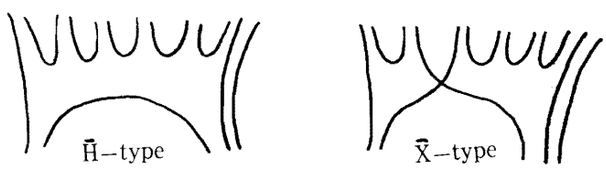

As discussed in this report, it seems to be natural to consider the ND type is dominant in the inelastic total cross section below $P_L \simeq 1$ TeV/c. Above 1 TeV region, the D mechanism may become dominant and then the multi-Pomeron exchange terms become important. This seems to be related to the $(\log s)^2$ behaviour of the pp total cross section mesuared recently at ISR.

Acknowledgement

The author would like to thank Dr. T. Morii for valuable discussions during this work. Also, useful discussions with the members of the research group 'Multi-Particle Production' organized by Research Institute for Fundamental Physics, Kyoto University, in 1973, are gratefully acknowledged.

References

1) T. Morii and H. Noda, Prog. Theor. Phys. 49 (1973), 2141 and 2143.
2) T. Morii and H. Noda, Kobe preprint (Kobe university) KULA-HP-73-1
3) D. Amati, S. Fubini and A. Stanghellini, Nuovo Cim. 26 (1962), 896 ; G. F. Chew and A. Pignotti, Phys. Rev. 176 (1968), 2112 ; J. Finkelstein and K. Kajantie, Nuovo Cim. 56A (1968), 659.
4) J. Beneche, T. T. Chou, C. N. Yang and E. Yen, Phys. Rev. 188 (1969), 2159 ; R. C. Hwa, Phys. Rev. Letters 26 (1971), 1143 ; M. Jacob and R. Slansky, Phys Letters 37B (1971), 408 and Phys. Rev. D5 (1972), 1847.
5) Y. Hama, Phys. Rev. D6 (1972), 3306.
6) S. Kagiyama, Prog. Theor. Phys. 49 (1973), 2031 ; H. Harari and E. Rabinovici, Phys. Letters 43B (1973), 49 ; K. Flalkowski and H. I. Miettinen, Phys. Letters 43B (1973), 61.
7) R. Honecker et al., Nuclear Phys. B13 (1969), 571.
8) M. Namiki, I. Ohba and Yap Sue-Pin, Prog. Theor. Phys. 47 (1972), 1247.
9) J. D. Hansen, W. Kittel and D. R. O. Morrison, Nuclear, Phys. B25 (1971), 605.
10) T. Morii and H. Noda, Prog. Theor. Phys. 50 (1973) No. 2
11) D. R. O. Morrison, Review of Quasi Two-body Reactions, Rapporteur's Talk given at the XV th International Conference on High Energy Physics, Kiev 1970.
12) M. Deutschmann et al., Nuclear Phys. B50 (1972), 61.
13) W. Burdett et al., Nuclear Phys. B48 (1972), 13
14) W. Kittel et al., Nuclear Phys. B30 (1971), 333.
15) H. Noda and K. Kinoshita, Prog. Theor. Phys. 48 (1972), 877.

Figure Captions

Fig. 1. The partial cross sections in π^- p collisions. The experimental data are taken from Ref. 7. (a) $\pi^- p \to \pi^- \pi^0 p$, (b) $\pi^- p \to \pi^- \pi^+ \pi^- p$, (c) $\pi^- p \to \pi^- \pi^+ \pi^- \pi^0 p$. The solid lines represent the contributions of ND and D mechanism and the dashed lines are the total contributions.

Fig. 2. The illustration of the band scheme on the multiplicity-incident momentum plane. Region (I): ND mechanism dominates; Region (II): ND and D mechanism are comparable to each other, and Region (III): D mechanism dominates.

Fig. 3. The multiplicity dependence of the momentum giving the maximum cross section.

Fig. 4. The rank structure of the partial cross section. The solid lines are obtained from ND mechanism, which are normarized at the rank number zero. The dotted lines show the further suppression by the exchange mechanism.

Fig. 5. The predicted energy development of the ratio of the occupation of σ_n (s) by the D mechanism. The shaded regions come from the D mechanism.

Fig. 6. The energy development of the N^* spectrum by the D_N mechanism.

Fig. 7. The energy development of the missing mass distribution by the ND mechanism.

Fig. 8. The energy development of the missing mass distribution by the D_π mechanism.

Fig. 9. The missing mass distribution of $\pi^- p \to \pi^-_f (m\pi + N)^+$ at $P_L = 16$ GeV/c from m = 1, 2, 3 and 4. The experimental data are taken from Ref. 11 and are shown in the dotted line. The solid lines represent the results calculated in our model by Monte Carlo method, and compose of the total sum of the contributions from all mechanisms, ND and D.

Fig. 10. The data of $\sigma_n^{(n+\cdot n-)}$. (a) $\pi^- p \to \pi^- \pi^+ \pi^- \pi^+ \pi^- p$, (b) $pp \to pp\pi^+ \pi^-$ and $pp \to pp\pi^+ \pi^- \pi^+ \pi^-$ at 28 GeV/c.

Fig. 11. The model calculation for $\sigma_n^{(n+\cdot n-)}$ of $\pi^- p \to \pi^- \pi^+ \pi^- p$ at 16 GeV/c and 64 GeV/c.

Fig. 12. The model calculation for $\frac{d\sigma_n}{dx_i}$ of $\pi^- p \to \pi^- \pi_3^+ \pi^-_2 p$ at 27 GeV/c.

Fig. 13. The model calculation for $\frac{d^2\sigma_n}{dx_2\, dx_3}$ of $\pi^- p \to \pi^-_f \pi_3 \pi_2 p$ at 16 GeV/c. and 64 GeV/c. The distribution develops from one peak to two peaks.

Fig. 14. The energy dependence of $\frac{d^2\sigma_n}{dx_2\, dx_3}$ predicted from our model at each sections ($|x_2| = |x_3| = 0.05$) and the contributions of each mechanisms.

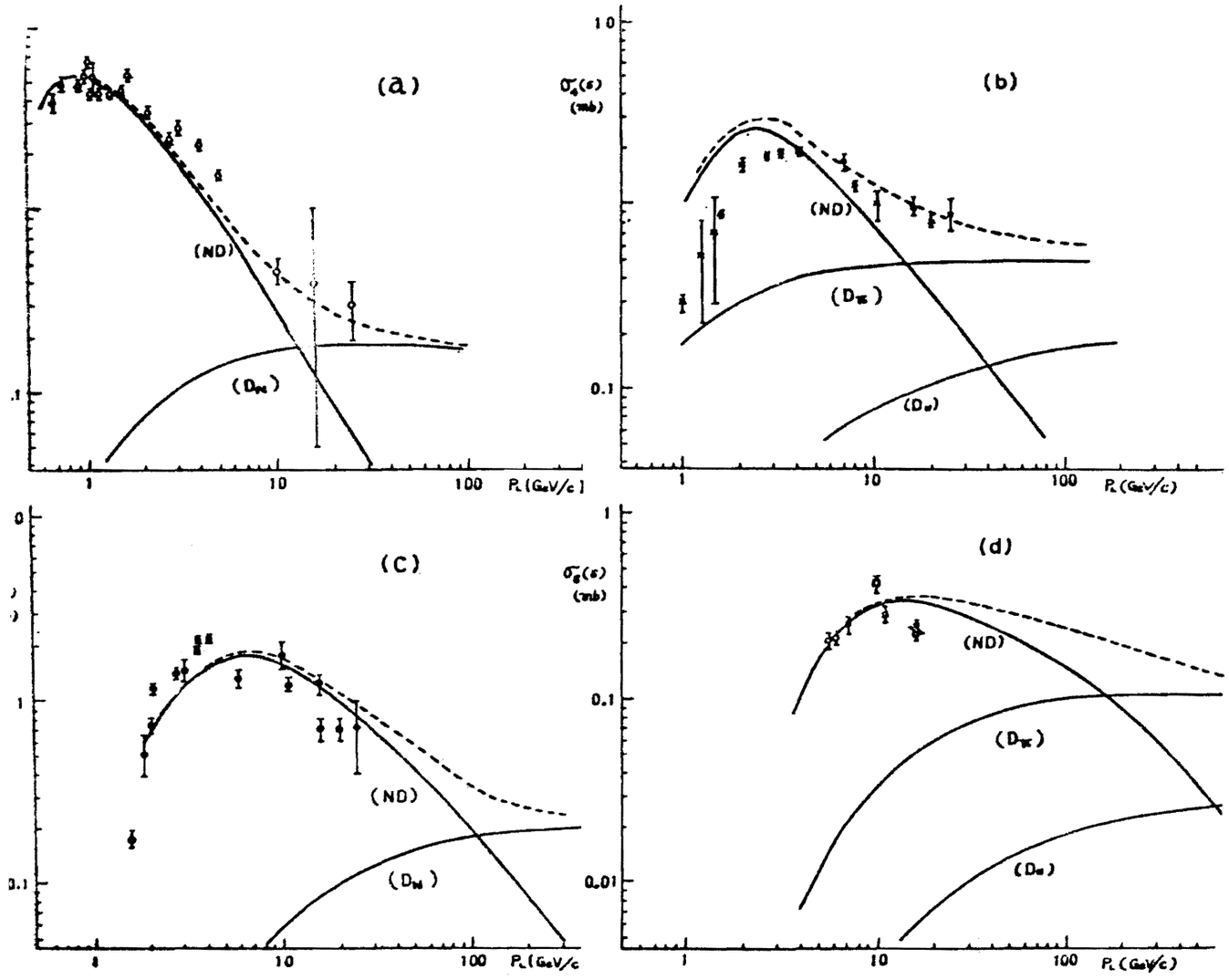

Fig. 1

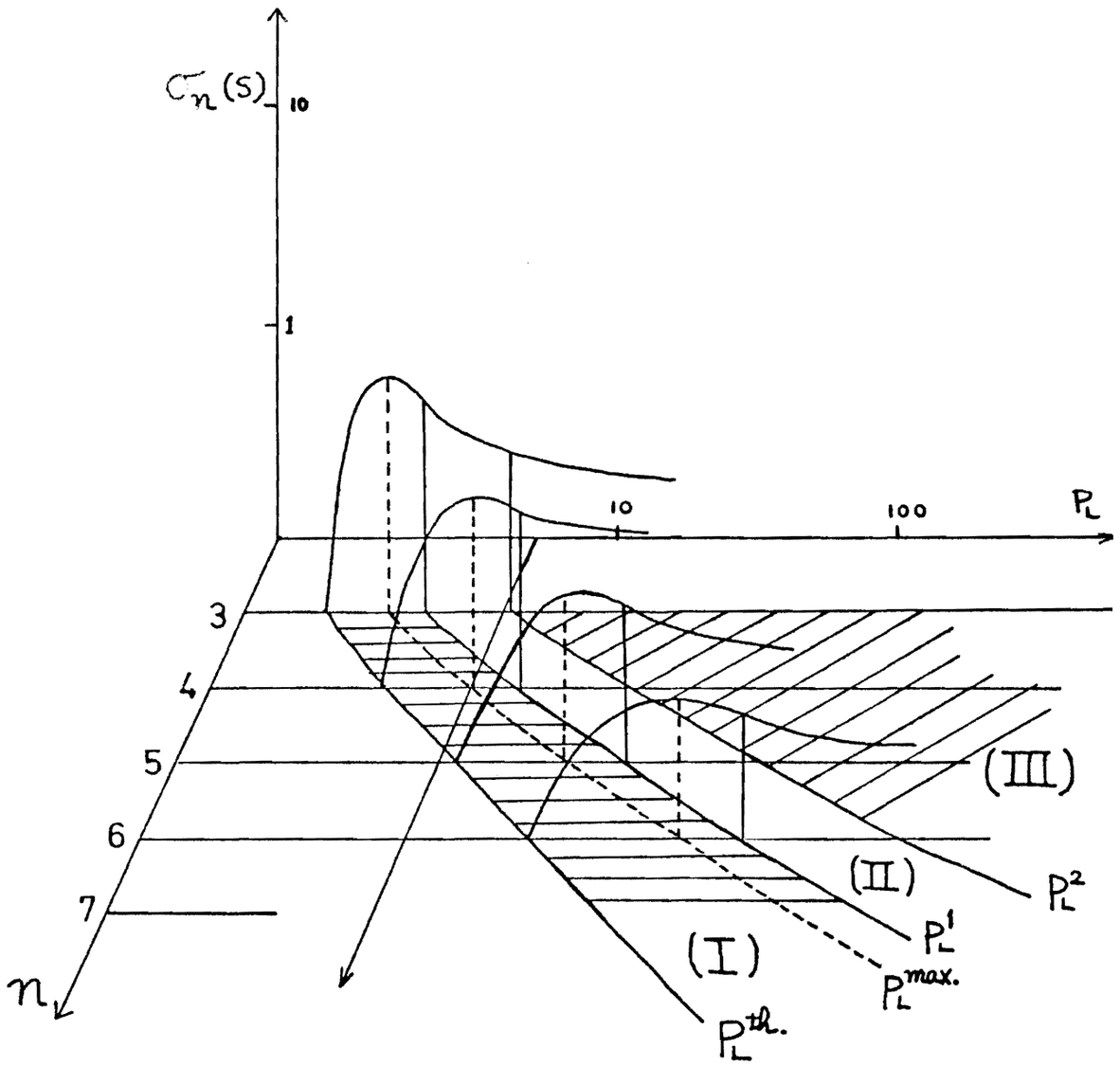

Fig. 2

Table 1

Values for A and B in the expression $P_n^{max.} = A n^B$ for πP, KP, PP reactions, respectively.

Initial Particles	A (GeV/c)		B	
	Theor.	Exp.*)	Theor.	Exp.*)
πP	0.030	0.067±0.025	2.9	2.5±0.2
KP	0.065	0.11±0.08	2.9	2.4±0.5
PP	0.095	0.13±0.05	2.9	2.6±0.2

*) Experimental values are from ref.

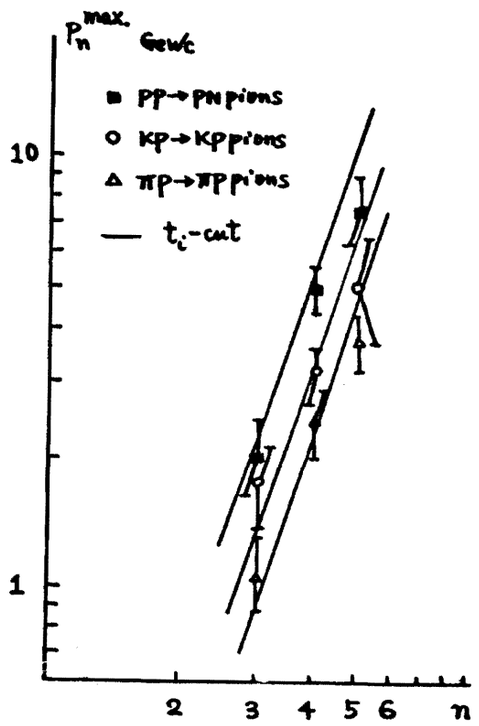

Fig. 3

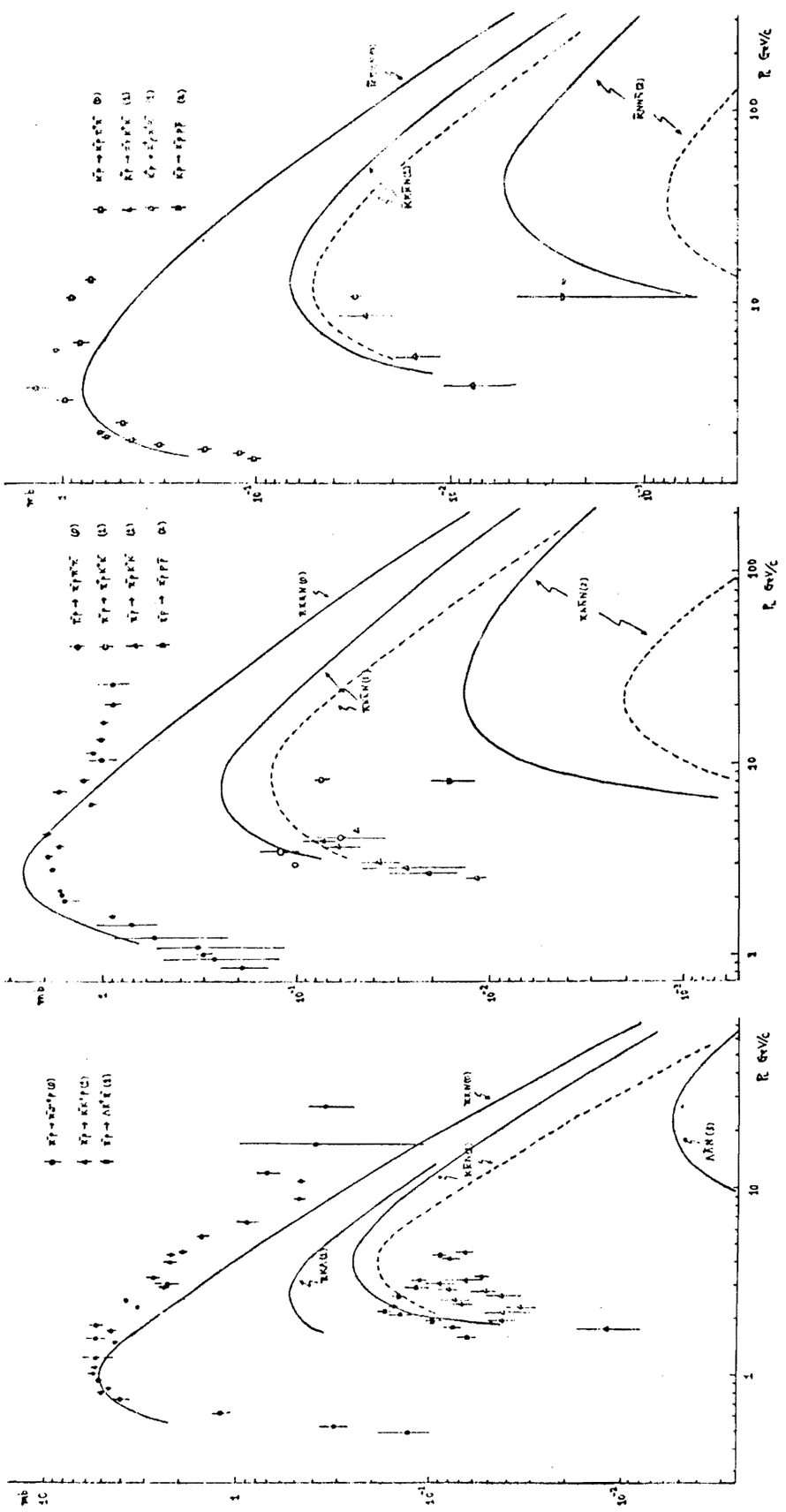

Fig.4

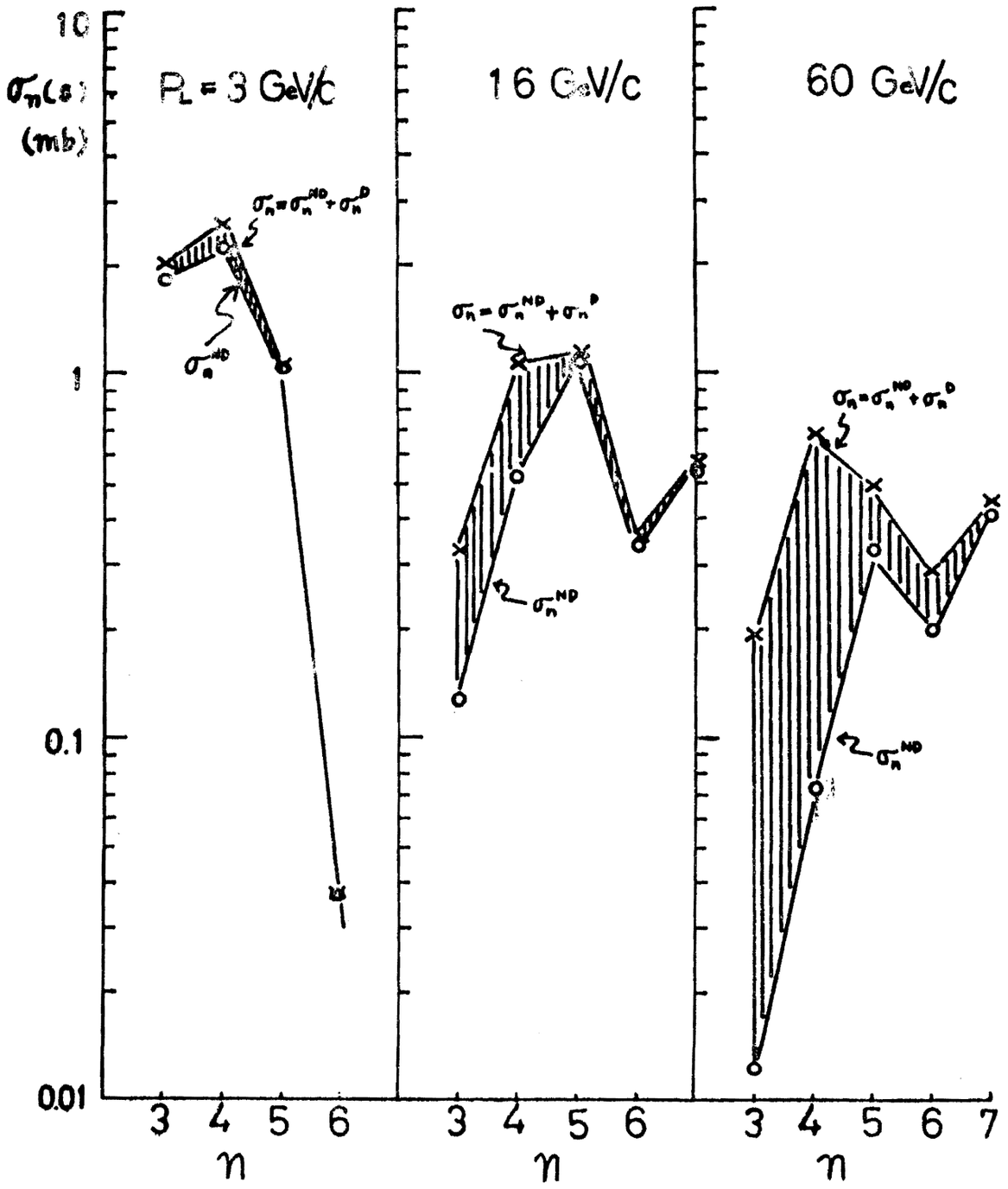
10
1
0.1
0.01
$\sigma_n(s)$
(mb)
P_L = 3 GeV/c
16 GeV/c
60 GeV/c
$\sigma_n = \sigma_n^{ND} + \sigma_n^{D}$
σ_n^{ND}
3 4 5 6
3 4 5 6
3 4 5 6 7
n
n
n

Fig.5

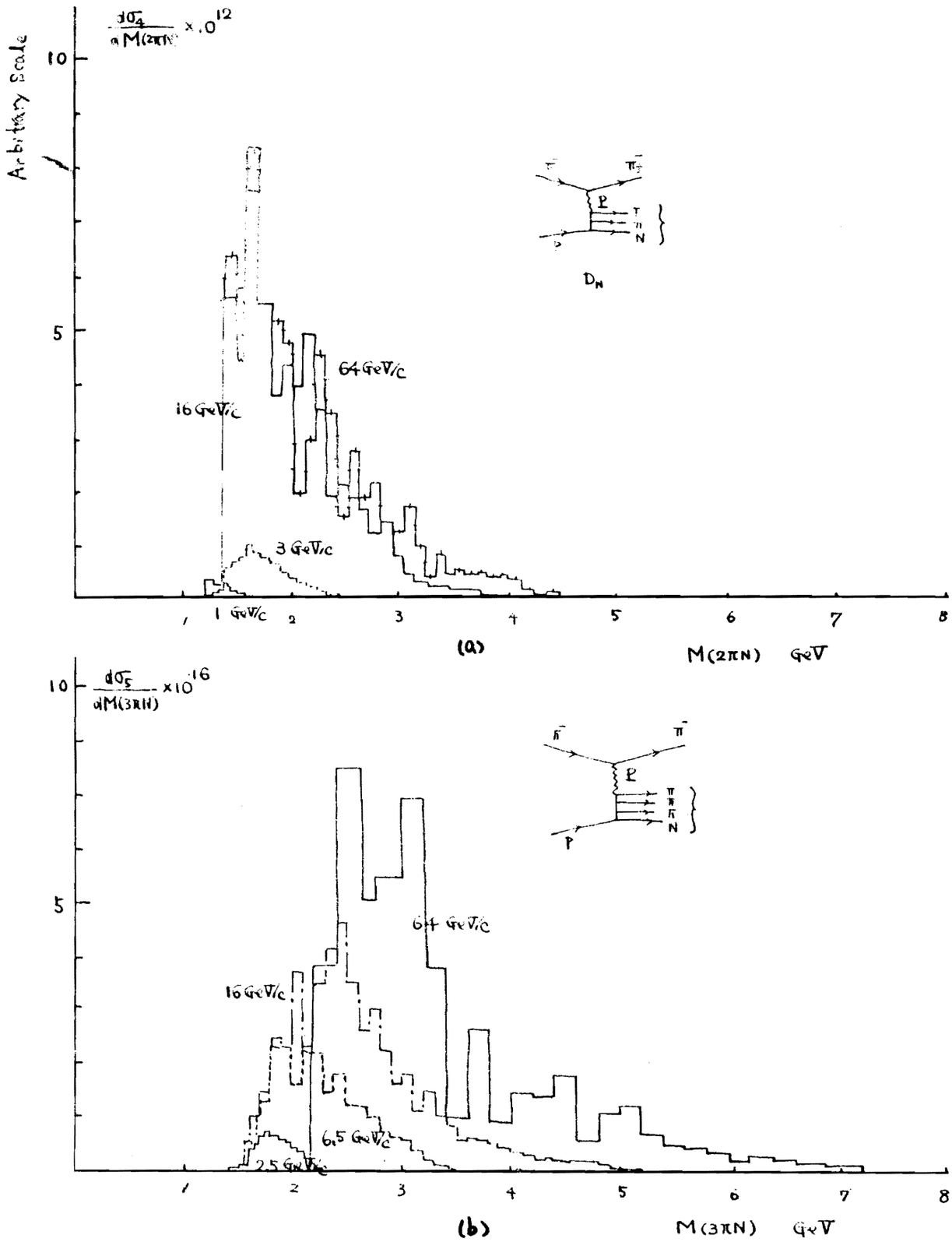
Arbitrary scale
10
5
64 GeV/c
16 GeV/c
3 GeV/c
1 GeV/c
1
2
3
4
5
6
7
8
(a)
M(2πN) GeV
D_N
10
5
64 GeV/c
16 GeV/c
6.5 GeV/c
2.5 GeV/c
(b)
M(3πN) GeV

Fig. 6

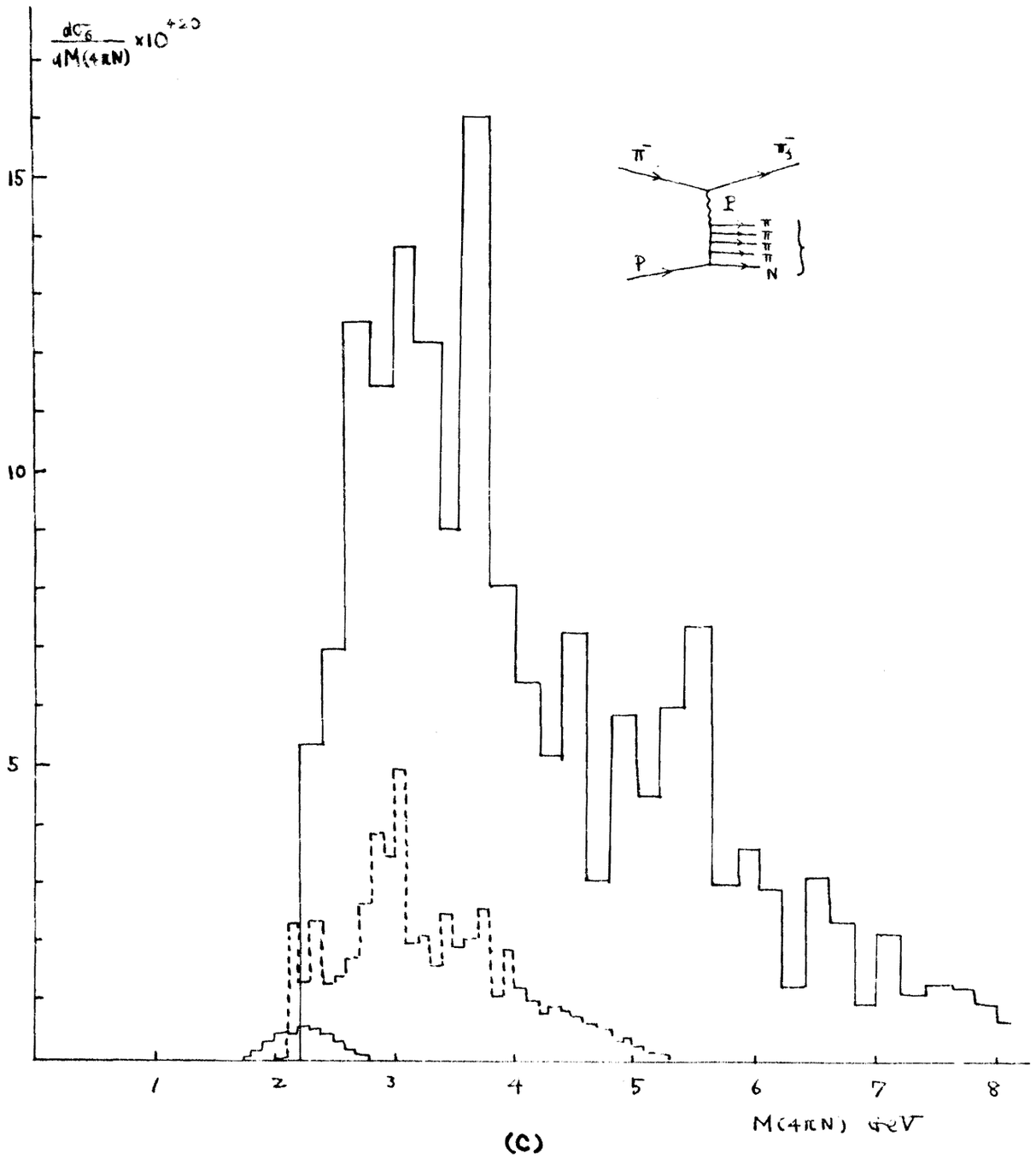

Fig. 6

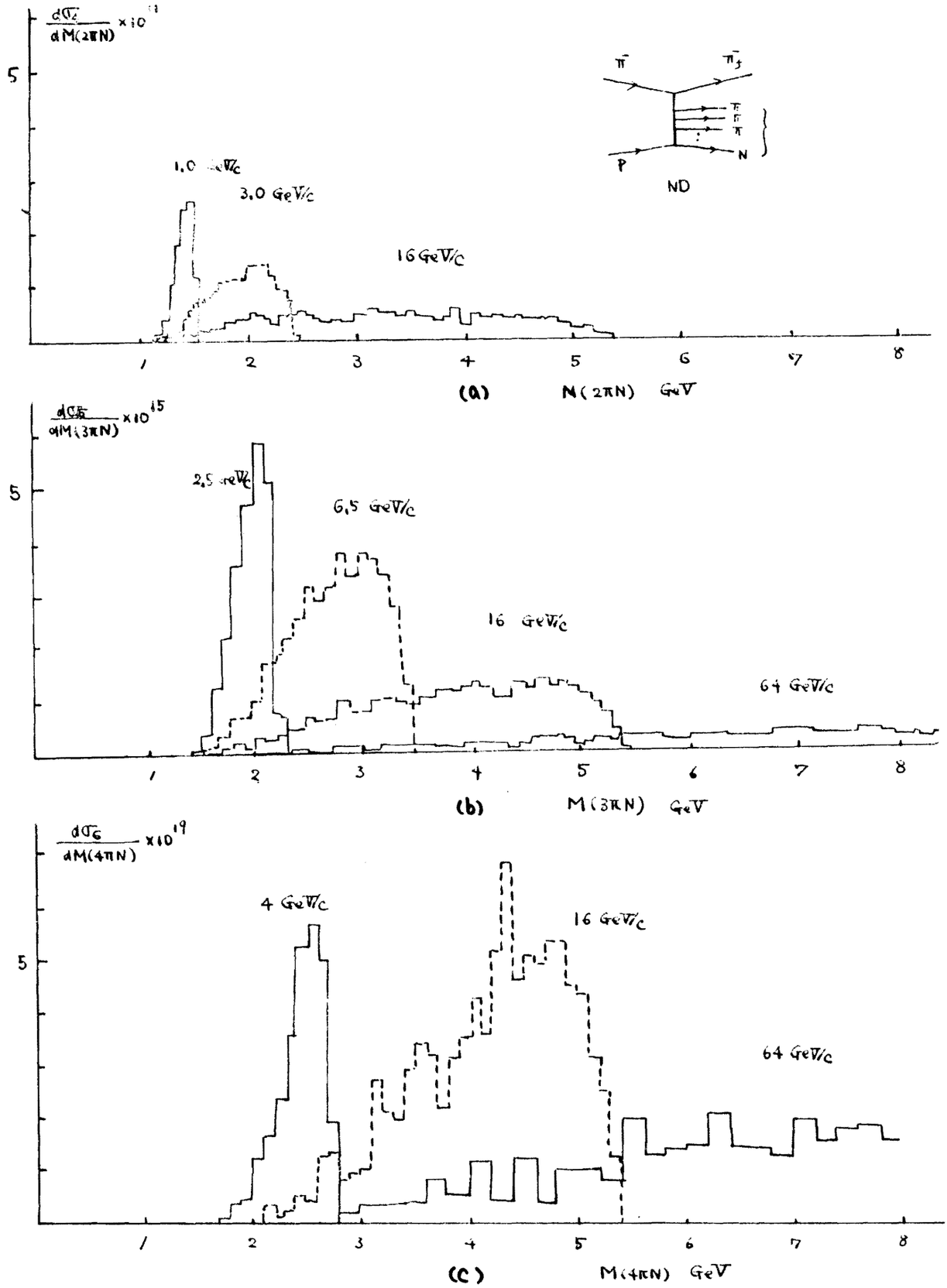
dσ_2/dM(2πN) ×10^33
5
1.0 GeV/c
3.0 GeV/c
16 GeV/c
ND
1 2 3 4 5 6 7 8
(a) N(2πN) GeV
dσ_3/dM(3πN) ×10^35
5
2.5 GeV/c
6.5 GeV/c
16 GeV/c
64 GeV/c
1 2 3 4 5 6 7 8
(b) M(3πN) GeV
dσ_4/dM(4πN) ×10^39
5
4 GeV/c
16 GeV/c
64 GeV/c
1 2 3 4 5 6 7 8
(c) M(4πN) GeV

Fig.7

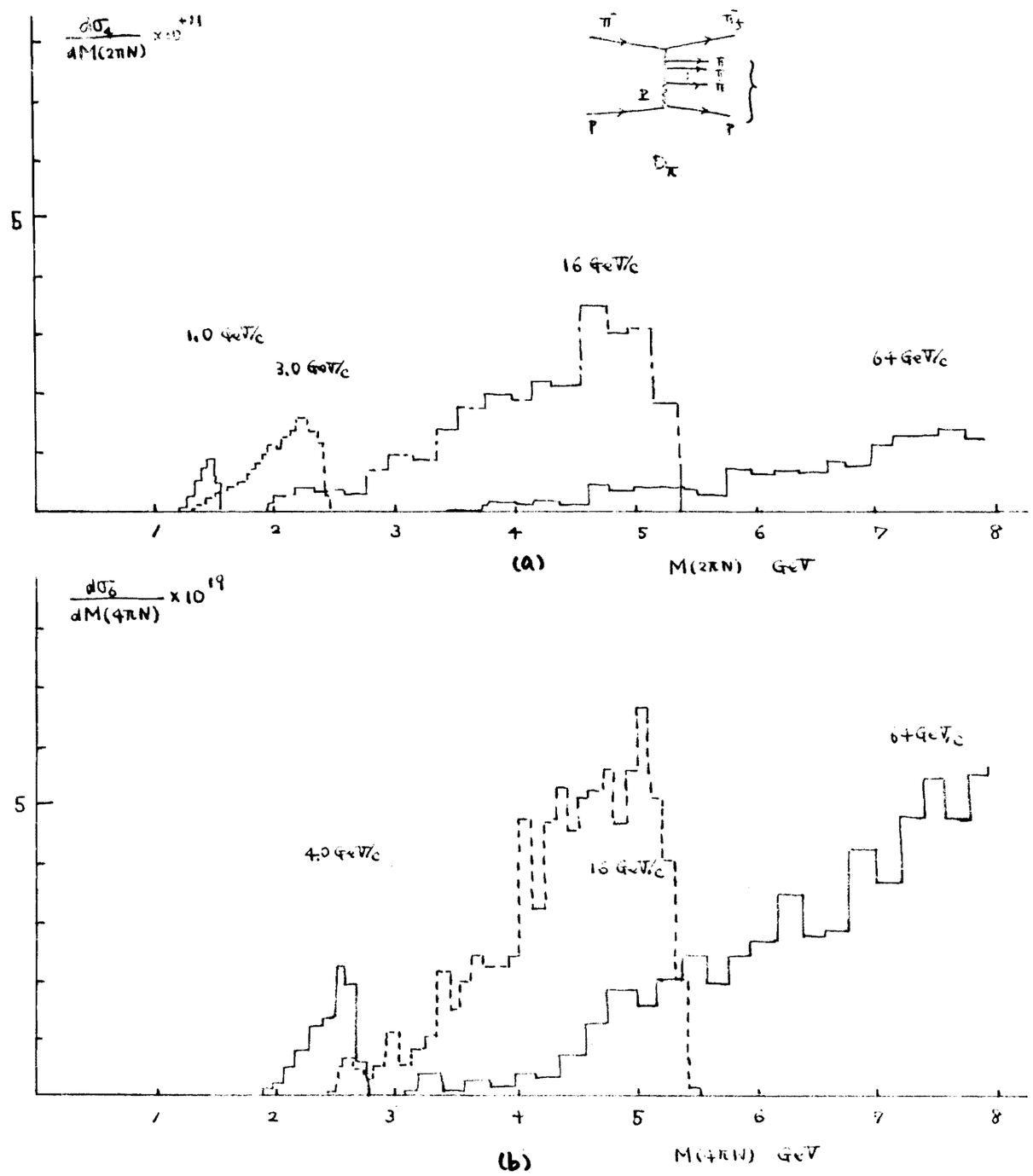
dσ/dM(2πN)
1.0 GeV/c
3.0 GeV/c
16 GeV/c
64 GeV/c
M(2πN) GeV
(a)
dσ/dM(4πN) x10^19
4.0 GeV/c
16 GeV/c
64 GeV/c
M(4πN) GeV
(b)

Fig.8

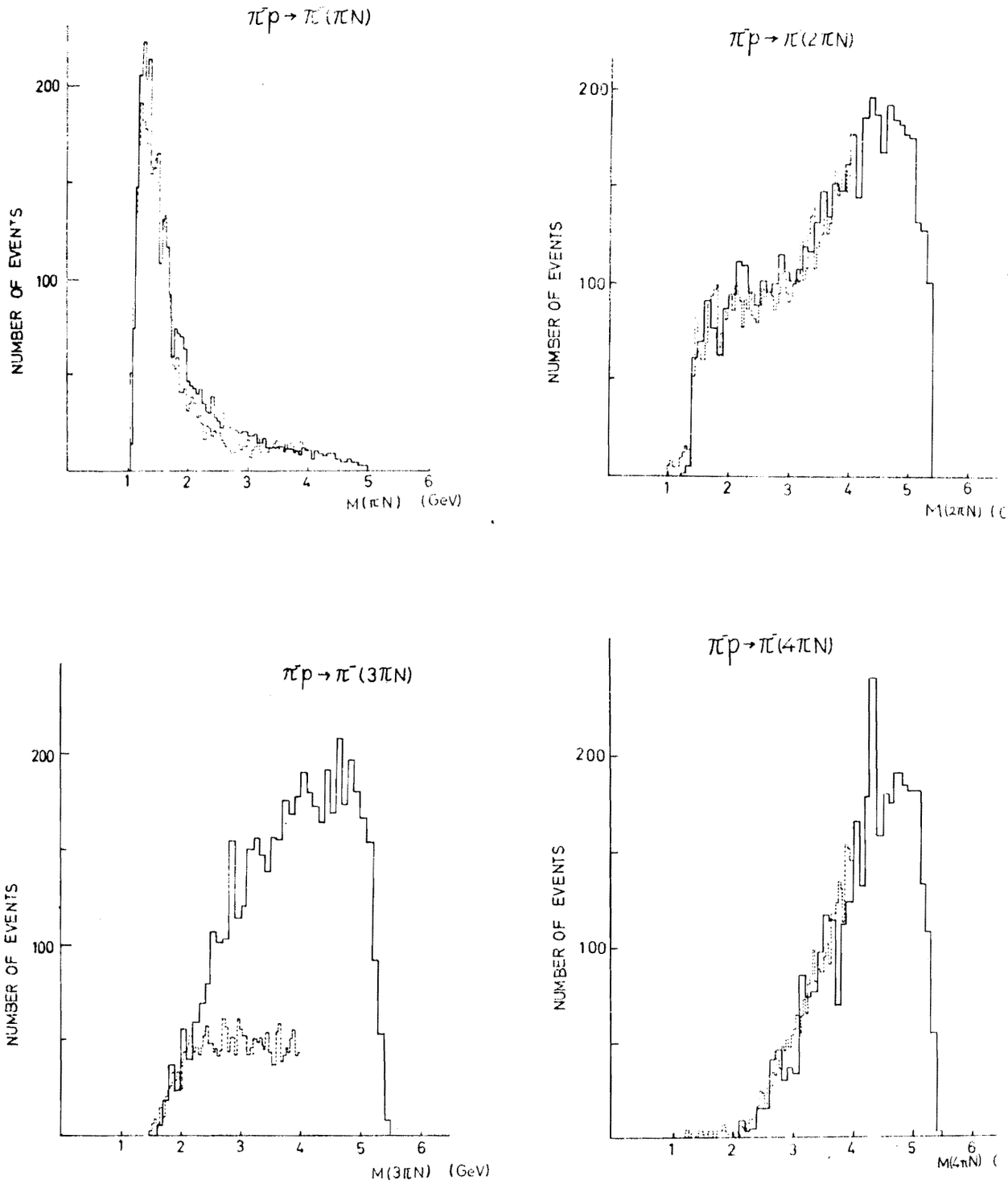
$\pi^- p \to \pi^-(\pi N)$
NUMBER OF EVENTS
200
100
1
2
3
4
5
6
M(πN) (GeV)
$\pi^- p \to \pi^-(2\pi N)$
NUMBER OF EVENTS
200
100
1
2
3
4
5
6
M(2πN)
$\pi^- p \to \pi^-(3\pi N)$
NUMBER OF EVENTS
200
100
1
2
3
4
5
6
M(3πN) (GeV)
$\pi^- p \to \pi^-(4\pi N)$
NUMBER OF EVENTS
200
100
1
2
3
4
5
6
M(4πN)

Fig. 9

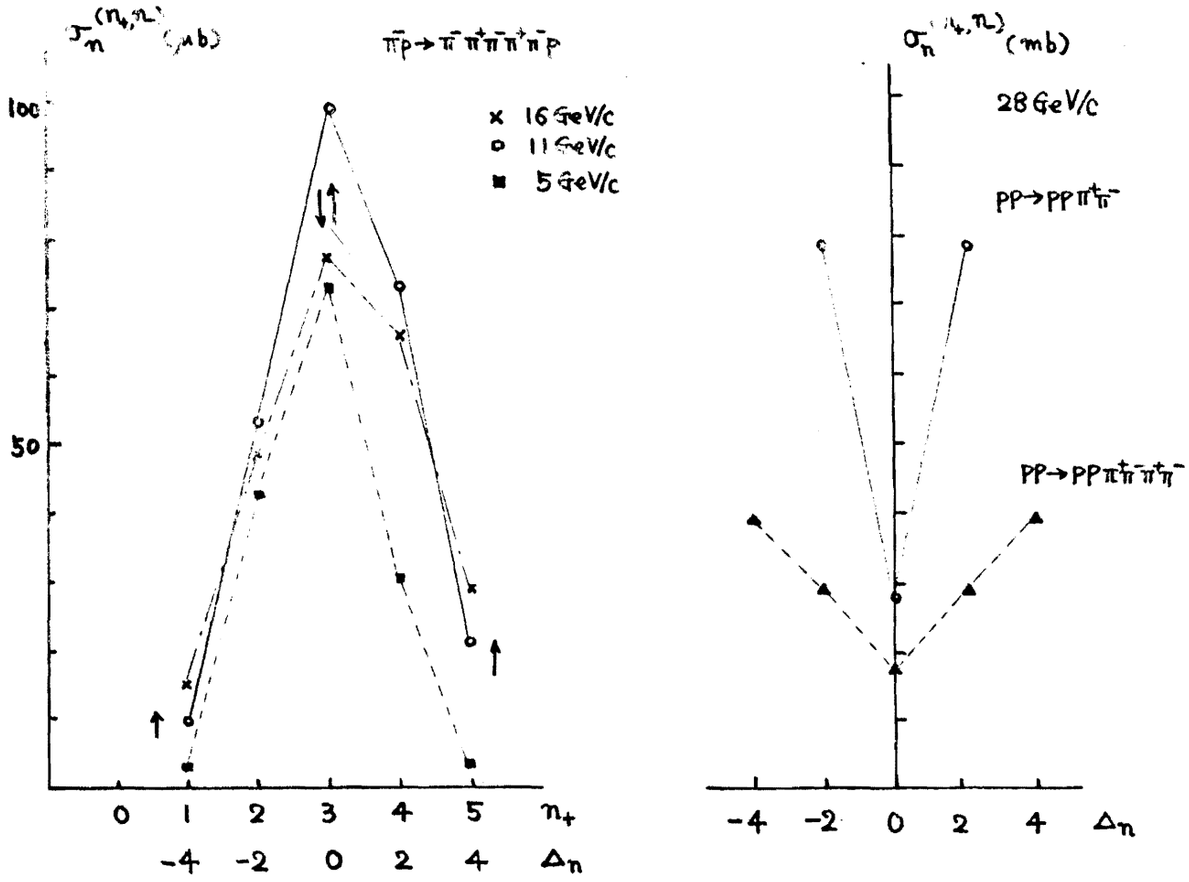
$\sigma_n^{(n_+,n_-)}$ (μb)
$\pi^- p \to \pi^-\pi^+\pi^-\pi^+\pi^- p$
× 16 GeV/c
○ 11 GeV/c
■ 5 GeV/c
100
50
0 1 2 3 4 5 n_+
-4 -2 0 2 4 Δn
$\sigma_n^{(n_+,n_-)}$ (mb)
28 GeV/c
$pp \to pp\pi^+\pi^-$
$pp \to pp\pi^+\pi^-\pi^+\pi^-$
-4 -2 0 2 4 Δn

Fig. 10

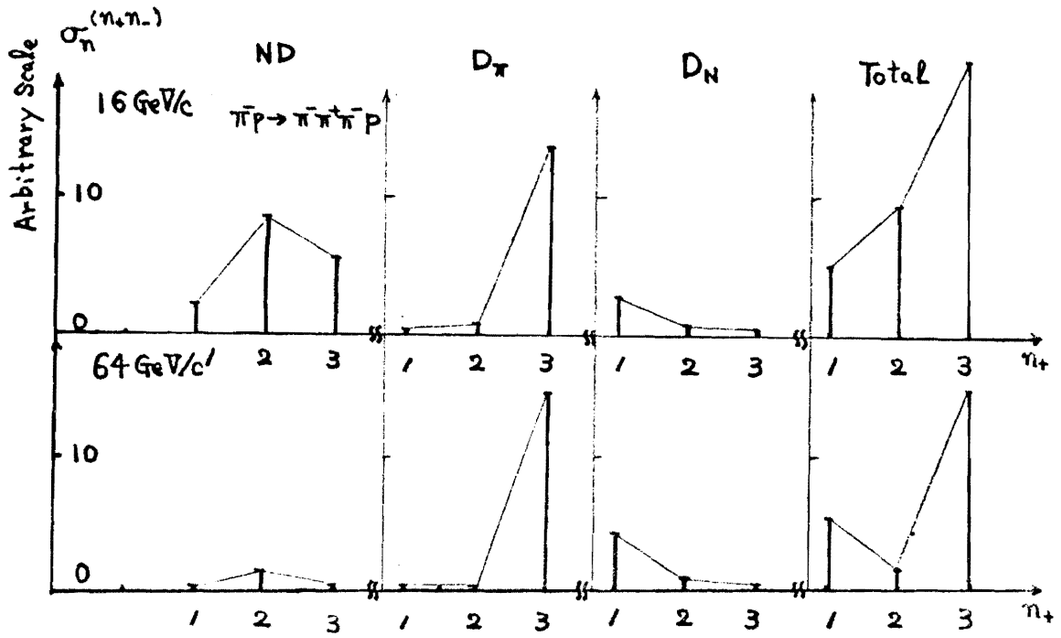
$\sigma_n^{(n_+,n_-)}$
Arbitrary Scale
ND
D_π
D_N
Total
16 GeV/c
$\pi^- p \to \pi^-\pi^+\pi^- p$
10
0
64 GeV/c
1 2 3
n_+

Fig. 11

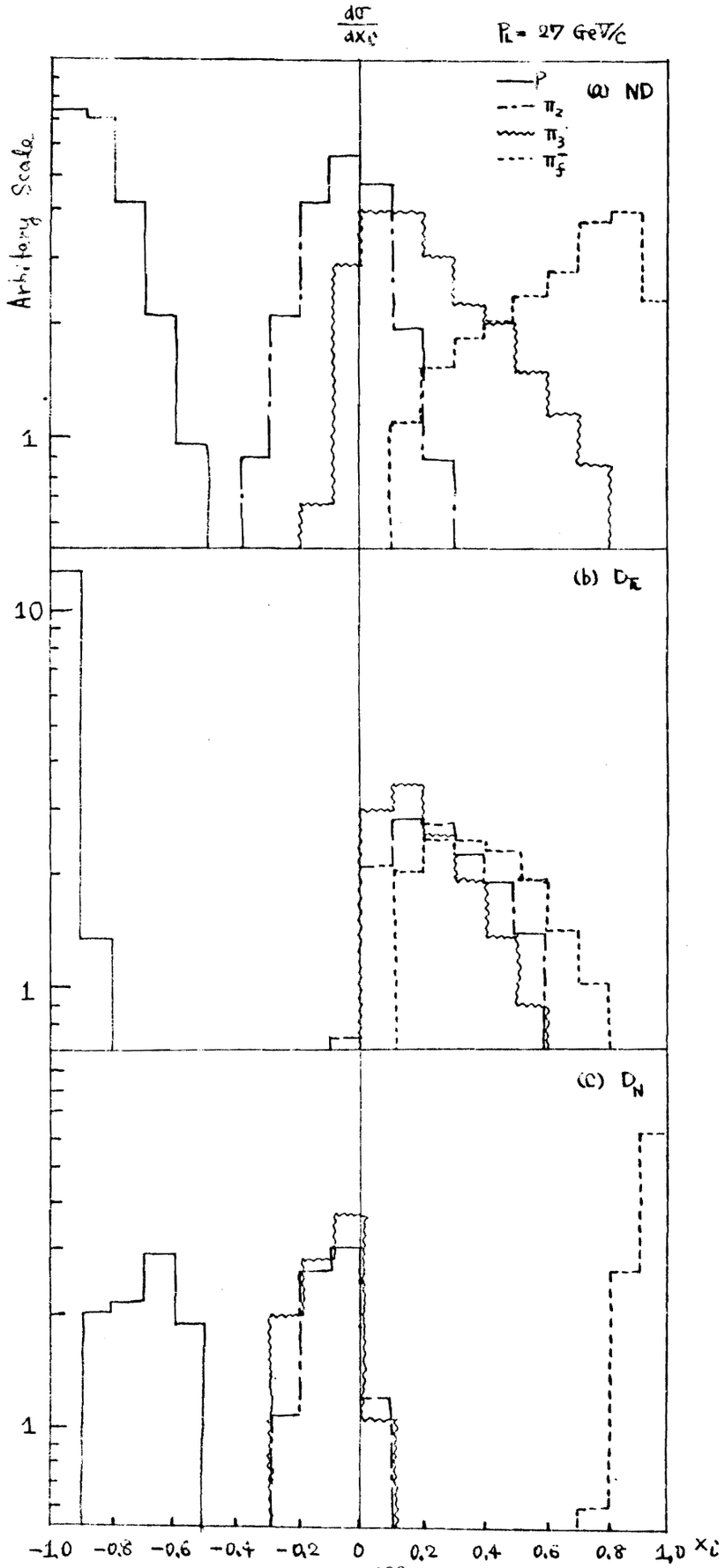
dσ/dx_i
P_L = 27 GeV/c
P
π+
π3
π−
(a) ND
Arbitrary Scale
1
(b) D_K
10
1
(c) D_N
1
-1.0 -0.8 -0.6 -0.4 -0.2 0 0.2 0.4 0.6 0.8 1.0 x_i

Fig. 12

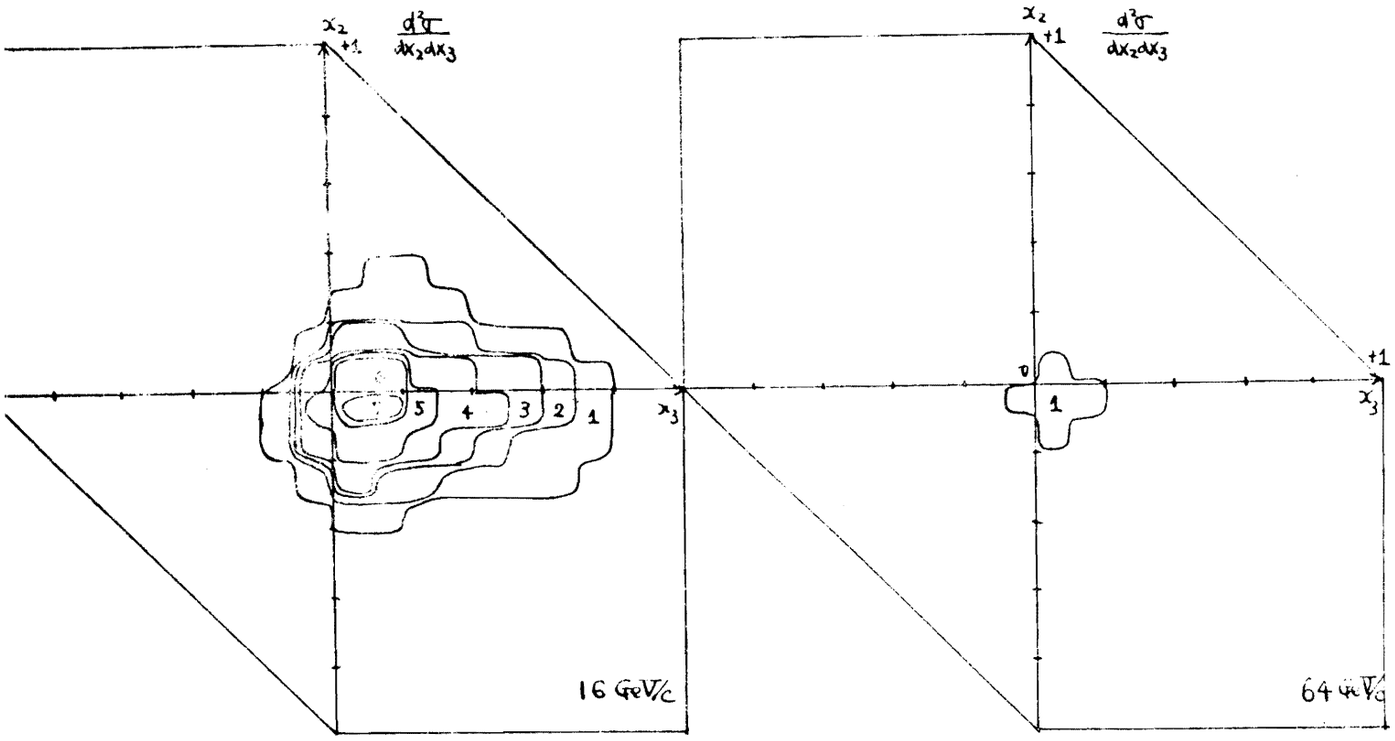

(A) ND

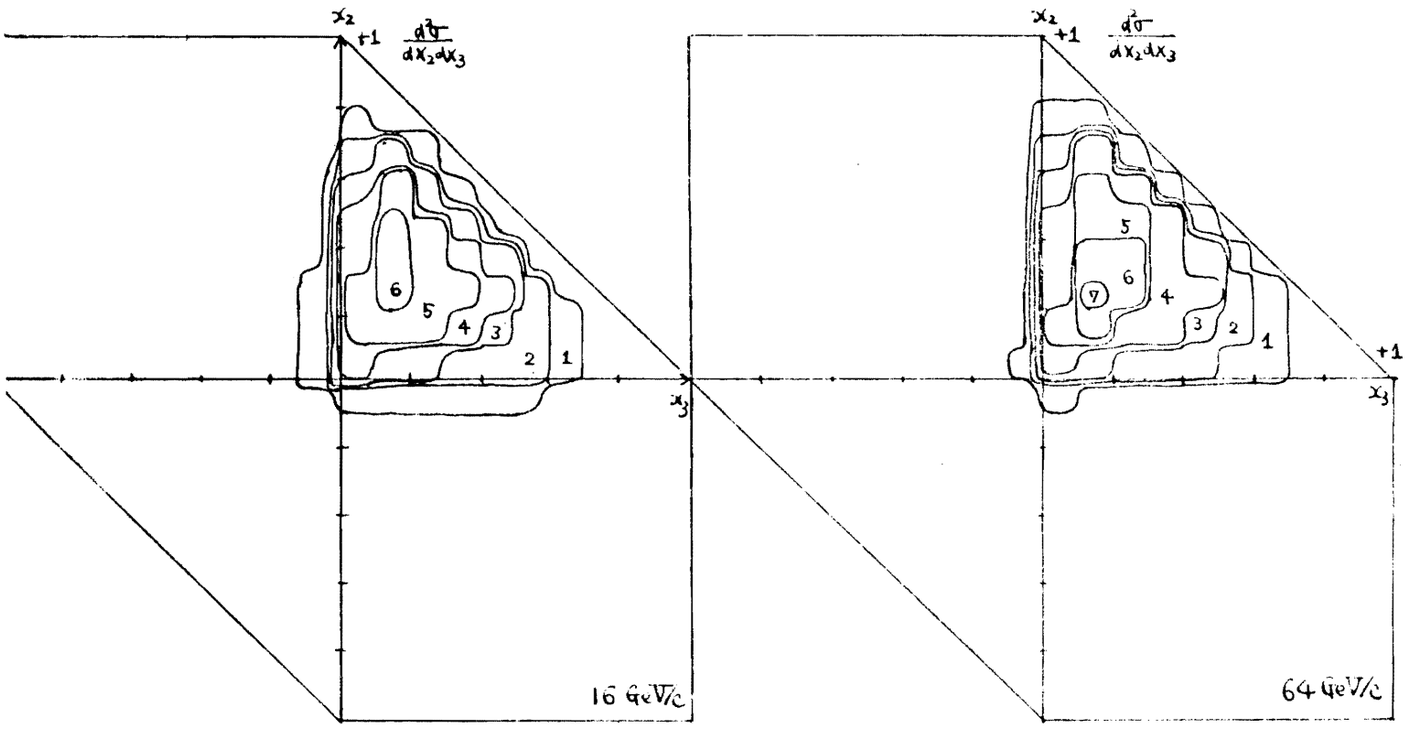

(B) D_{11}

Fig. 13

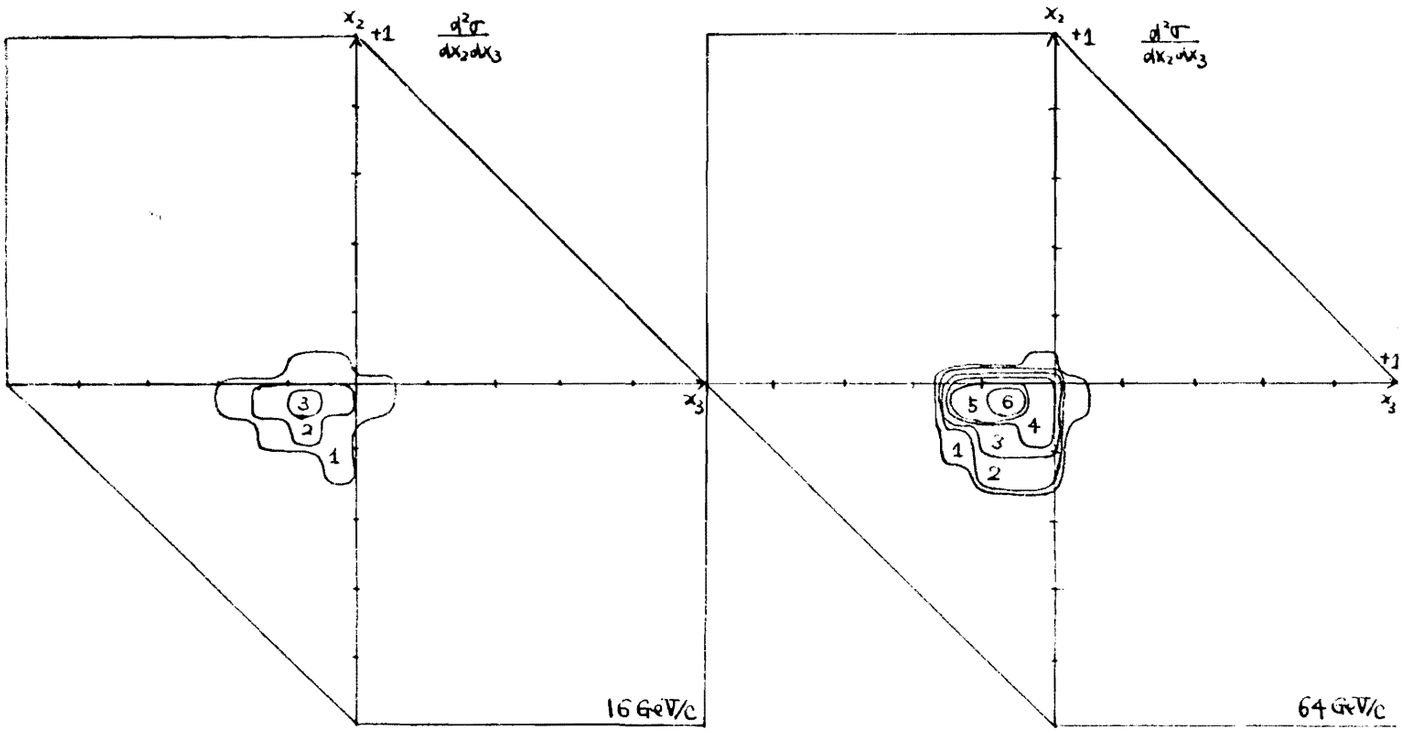

(c) D_N

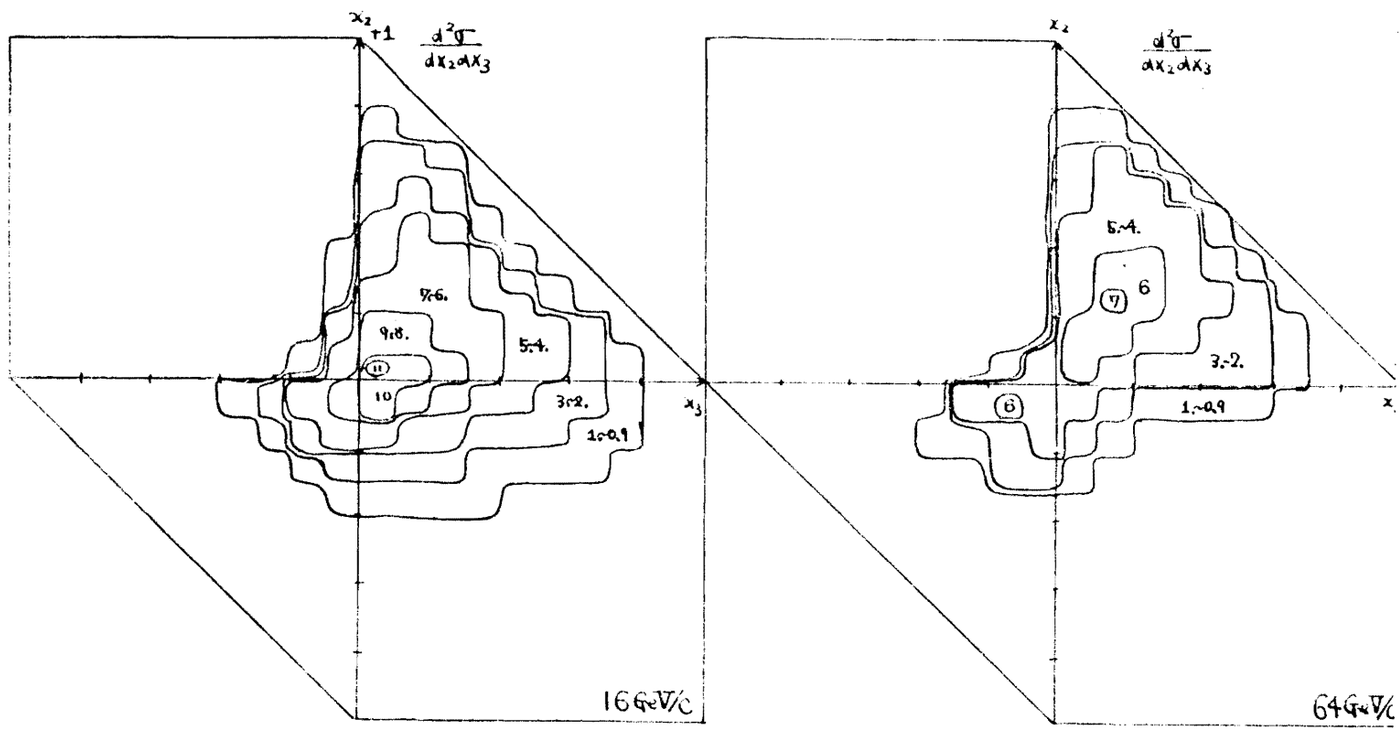

(D) Total

Fig. 13

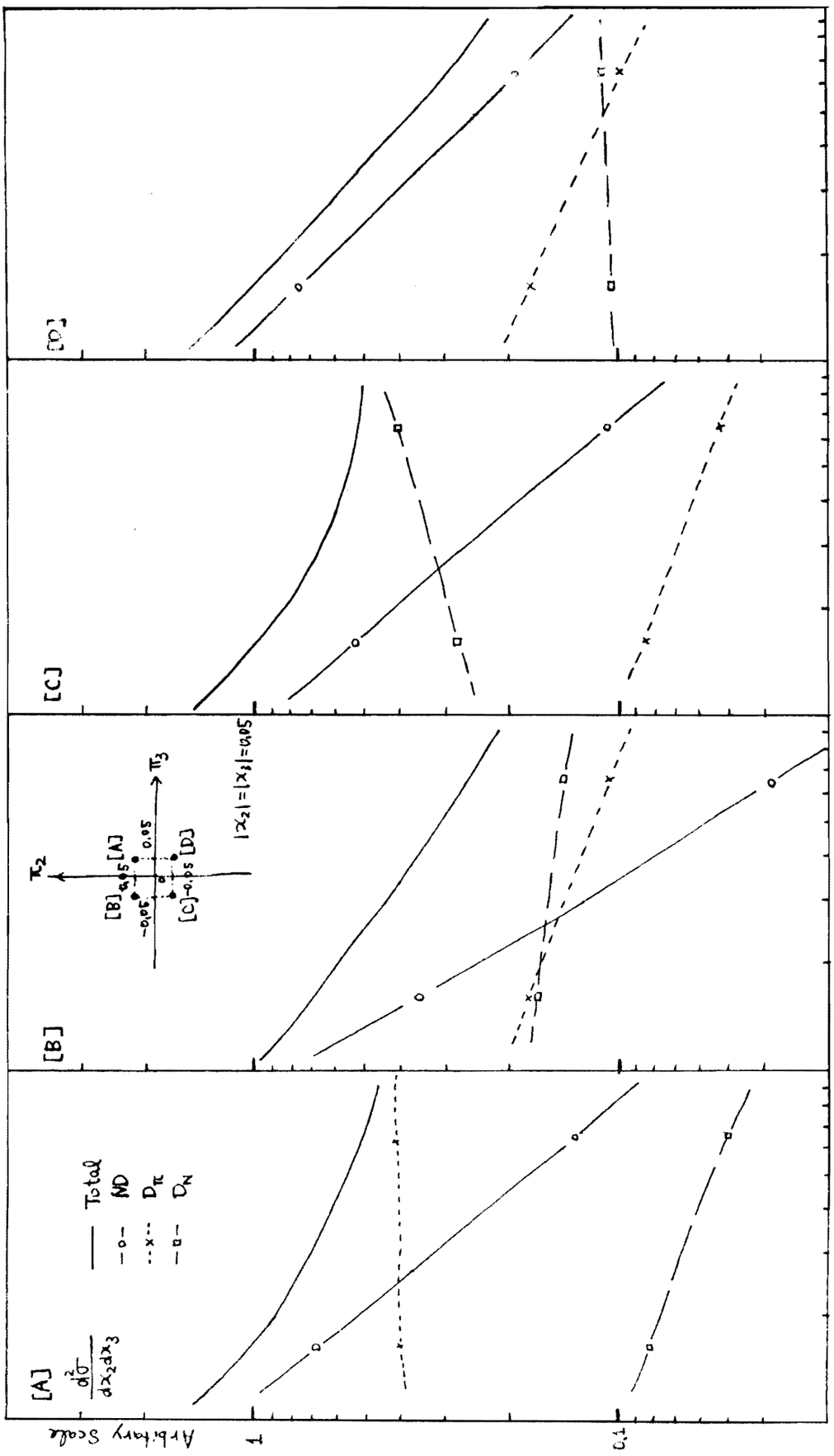
[A]
$\frac{d^2\sigma}{dx_2 dx_3}$
Total
MD
D_π
D_N
Arbitrary Scale
1
0.1
10 GeV/c
[B]
x_2
x_3
[A]
[B]
[C]
[D]
0.05
-0.05
$|x_2|=|x_3|=0.05$
10 GeV/c
P_L
[C]
10 GeV/c

Fig. 14